Icarus **148**, 2–11 (2000)
doi:10.1006/icar.2000.6485, available online at http://www.idealibrary.com on IDEAL®

Radiative Spin-up and Spin-down of Small Asteroids

David Parry Rubincam

Geodynamics Branch, Code 921, Laboratory for Terrestrial Physics, NASA's Goddard Space Flight Center, Greenbelt, Maryland 20771
E-mail: rubincam@denali.gsfc.nasa.gov

Received June 18, 1999; revised October 27, 1999

The Yarkovsky–O'Keefe–Radzievskii–Paddack (YORP) effect may spin up or spin down 5-km-radius asteroids on a 10^8-year timescale. Smaller asteroids spin up or down even faster due to the radius-squared dependence of the YORP timescale. The mechanism is the absorption of sunlight and its re-emission as thermal radiation from an irregularly shaped asteroid. This effect may compete with impacts and tidal encounters as a way of changing rotation rates for small asteroids, especially in the near-Earth region. The YORP effect may explain the rapid rotation of 1566 Icarus and the slow tumbling of 4179 Toutatis. It may explain to some extent the slow rotation of 253 Mathilde. Meteoroids spin up or down on timescales fast compared to their cosmic ray exposure ages.

Key Words: **asteroids, rotation; meteoroids; asteroids, Eros; asteroids, Gaspra; surfaces, Asteroid.**

INTRODUCTION

The major mechanism for changing the spin state of small asteroids is generally thought to be collisions (Davis *et al.* 1989) and tidal encounters (Bottke *et al.* 1997, Richardson *et al.* 1998), but thermal torques, one aspect of the Yarkovsky–O'Keefe–Radzievskii–Paddack effect, may also be important for kilometer- and smaller-sized asteroids, especially in the near-Earth region. It has been known for some time that another aspect of this effect (YORP effect for short), namely sunlight reflecting off a body with an appropriate shape, can spin up small bodies orbiting the Sun (Radzievskii 1954, Paddack 1969, 1973, Paddack and Rhee 1975, O'Keefe 1976, Sazanov 1994, Komarov and Sazanov 1994). The reflection can transfer angular momentum to the body, causing it to change its rotation speed. One example of such a shape is a propeller, with the Sun on the rotation axis; sunlight bouncing off the blades would cause it to spin. The amount of torque imparted to an object is tiny, due to the small amount of momentum carried by photons. However, the YORP torque is secular, so that after a long period of time the body's rotation rate can be substantially altered.

In the Yarkovsky–O'Keefe–Radzievskii–Paddack effect, thermal emission of infrared radiation from a body can also produce a torque, so that even a nonreflective blackbody can be spun up if it has the right shape. This is significant, since small Solar System objects tend to be very dark (e.g., Tedesco 1989). These thermal torques, part of the YORP effect, can substantially alter the rotation rate of 10-km-diameter asteroids on a 10^8-year timescale for suitable shapes. Smaller asteroids and meteoroids spin up or down even faster.

The principle of thermal torqueing due to the Yarkovsky–O'Keefe–Radzievskii–Paddack effect is illustrated in Fig. 1, which shows a rotating spherical asteroid with two identical wedges attached to its equator. The asteroid is assumed to be a blackbody, with the Sun lying in the asteroid's equatorial plane. Also, the asteroid's center of mass is assumed to be at the center of the sphere. The Sun heats the surface; this energy is reemitted as thermal radiation. Since photons carry momentum, as thermal photons leave the surface they impart a kick to the asteroid by momentum conservation. It is assumed here that the photons departing from any given spot on the surface obey Lambert's law, which means that they are axially distributed about the local vertical, giving a net downward force perpendicular to the surface. There will be no radiative torque on the spherical part of the asteroid because forces on the sphere point to the center of mass; they have no lever arm. Hence only the forces on the wedges need be considered.

As the asteroid rotates around, the Sun shines on the vertical face of one wedge and the slanted face of the other. At the instant shown in the figure, each wedge intercepts the same amount of sunlight; if it reradiates all of this energy thermally, there will be a net torque on the asteroid. The reason is that though the magnitude of the force on each face is the same, the forces do not cancel; each force is normal to its surface (see Fig. 2). The equatorial component of force on the slanted face is smaller than the force on the vertical face, causing a net torque along the rotation axis. This thermal torque does not average to zero as the asteroid rotates through 360°, so that there is a secular component. The asteroid spins faster and faster over time.

A body must have a certain amount of "windmill" asymmetry in its shape, like the asteroid in Fig. 1, to be spun up (Paddack 1969, 1973, Paddack and Rhee 1975, O'Keefe 1976); figures of revolution or even triaxial ellipsoids will not suffer from the YORP effect. There will also be an instantaneous torque from the sunlight striking the surface and being absorbed by the blackbody asteroid. This torque will average to zero because it depends on the silhouette that the asteroid presents to the Sun; the

0019-1035/00 $35.00

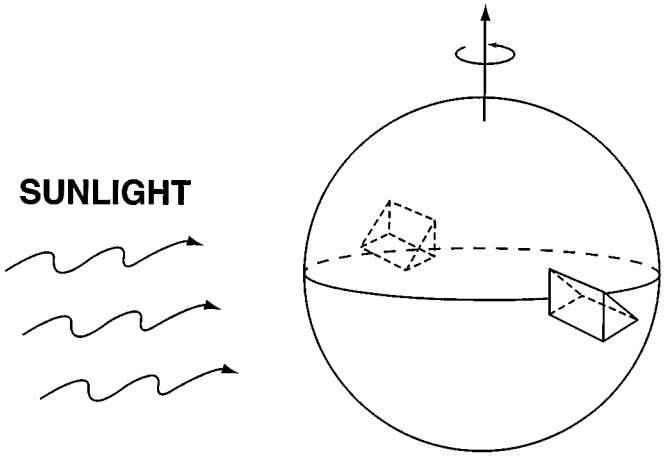

FIG. 1. Spin-up of an asymmetrical asteroid. The asteroid is modeled as a sphere with two wedges attached to its equator. The asteroid is a blackbody, so that it absorbs all the sunlight falling upon it. The solar energy is reemitted as thermal radiation, which causes a net torque on the asteroid.

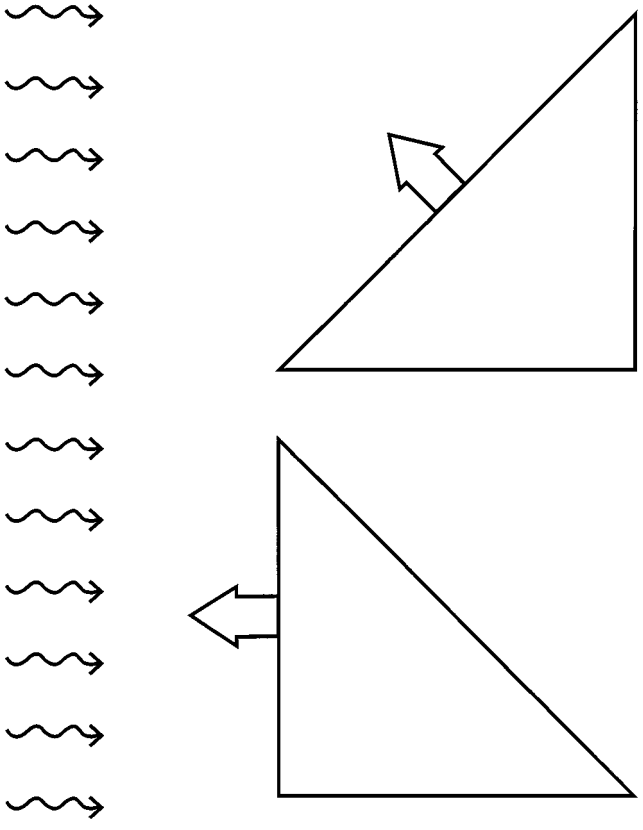

FIG. 2. The radiative forces on the wedges. Sunlight (wavy arrows) comes in horizontally from the left. Each surface absorbs the same amount of sunlight and reradiates in the infrared according to Lambert's law. The net momentum of the photons departing the surface is normal to the surface (thick arrows). By action–reaction, the wedge is kicked in the opposite direction. There is a net torque about the rotation axis because each force has the same magnitude but different directions.

solar torques will cancel themselves as the Sun sees the silhouette in all aspects.

PSEUDO-ASTEROIDS

The thermal torques from the YORP effect are computed below on the five hypothetical asteroids Pseudo-gaspra, Pseudo-ida, Pseudo-eros, Pseudo-phobos, and Pseudo-deimos. They are so-called because their shapes are based on spherical harmonic expansions of the real shapes of asteroids 951 Gaspra, 243 Ida, and 433 Eros, as well as Phobos and Deimos (the two moons of Mars). Their sizes are allowed to vary, but the shapes and densities stay the same. Each is a blackbody. They are taken to be in circular orbits about the Sun. Pseudo-gaspra orbits the Sun at 2.21 AU, just as the real Gaspra does; likewise Pseudo-ida orbits at 2.86 AU while Pseudo-eros orbits at 1.46 AU, like the actual asteroids do. Pseudo-phobos and Pseudo-deimos are taken to circle the Sun at 3 AU, in order to place them in the main asteroid belt. These objects have been chosen because numerical shapes have been determined for them by P. Thomas (Thomas *et al.* 1994, 1996, Rubincam *et al.* 1995) and others (see Acknowledgments). Hence their shapes will be more realistic for (if not necessarily representative of) small asteroids than artificially concocted shapes.

Each pseudo-asteroid's shape is given by

$$r = \sum_{lmi}^{l_{\max}} A_{lmi} Y_{lmi}(\theta, \lambda), \tag{1}$$

where the spherical harmonics are

$$Y_{lm1}(\theta, \lambda) = P_{lm}(\cos\theta)\cos m\lambda$$
$$Y_{lm2}(\theta, \lambda) = P_{lm}(\cos\theta)\sin m\lambda,$$

with $P_{lm}(\cos\theta)$ being the associated Legendre polynomial of degree l and order m, while θ is colatitude and λ is east longitude. Here the A_{lmi} are the shape coefficients derived from inner products of spherical harmonics with the numerical shapes.

The thermal torques are computed numerically by finding the thermal force on $5^\circ \times 5^\circ$ squares of the spherical harmonic shape. The Sun shines on an asteroid with strength

$$F_S = F_E \left(\frac{a_E}{r_S}\right)^2, \tag{2}$$

where r_S is the asteroid's distance from the Sun, and $F_E = 1378\ \mathrm{W\ m^{-2}}$ at the Earth's distance $a_E = 1$ AU. The amount of solar power deposited on a surface element with area $\mathrm{d}A$ is then $S\mathrm{d}A = (\hat{\mathbf{r}}_S \cdot \hat{\mathbf{N}})F_S\mathrm{d}A$, where $\hat{\mathbf{r}}_S$ is the unit vector pointing from the asteroid to the Sun, $\hat{\mathbf{N}}$ is the unit vector normal to the surface element, and S is the insolation. If each surface element is in a radiative steady state with respect to the insolation, the blackbody temperature T of each square will be given by $\sigma T^4 = S$,

where σ is the Stefan-Boltzmann constant (e.g., Lebofsky and Spencer 1989, Rubincam 1995). For Lambert's law, the force $\mathbf{f}$ per unit area exerted by the reaction to the escaping photons is normal to the surface in the direction -$\hat{\mathbf{N}}$ and given by $2\sigma T^4/3c$, where c is the speed of light (see for example Rubincam 1987). Thus for this ideal situation the force per unit area on dA is

$$\mathbf{f} = -2(\hat{\mathbf{r}}_S \cdot \hat{\mathbf{N}})F_S\hat{\mathbf{N}}/3c. \tag{3}$$

This force is then reduced by a thermal fudge factor $f_{\rm th}$ to account for possible thermal inertia and conduction in the regolith. The variation in temperature ΔT behaves like

$$\Delta T \propto [1 + 2\Phi + 2\Phi^2]^{-\frac{1}{2}} \tag{4}$$

in a linearized theory (Rubincam 1995, p. 1587), where Φ is half the thermal parameter of Lebofsky and Spencer (1989). Asteroids rotate typically rotate with periods near 12 h (e.g., Binzel *et al.* 1989). Using the conductivity and density of the lunar regolith gives $\Phi \cong 0.4$ at 3 AU for a rapid 6-h rotation period (Rubincam 1995, pp. 1587 and 1591). From (4) these considerations produce a conservative fudge factor of $f_{\rm th} \cong \frac{2}{3}$. Clearly by proceeding in this simple way the actual temperature T need not be solved for; computing the insolation S is all that is needed. These calculations could obviously be refined further, but this is unnecessary here, since this paper is concerned only with demonstrating the order-of-magnitude of YORP.

The elemental torque d$\boldsymbol{\tau}$ on the surface element is given by

$$\mathrm{d}\boldsymbol{\tau} = \mathbf{r} \times \mathbf{f}\,\mathrm{d}A, \tag{5}$$

where $\mathbf{r}$ is the distance from the center-of-mass to dA. All of the elemental torques are summed up to find the total torque about the rotation axis. The center-of-mass is found from the asteroid's shape, assuming a uniform density. The torque is determined for every 5° of rotation and averaged over one full rotation of the asteroid on its axis and over one full revolution as it orbits the Sun.

Shadowing is included in the calculations on all the pseudo-asteroids. The coordinate system is rotated so that the Sun shines down the new z-axis. Starting from colatitude zero and a given longitude in the new system, colatitude is increased and each $5^\circ \times 5^\circ$ square is checked to see if some previous square at the same longitude juts out further from the z-axis. If so, the present square is in shadow and the force on it is set to zero. Otherwise it is in sunlight and the torque is calculated as described previously. The normal to the surface, which gives the direction opposite to the force on the surface, is found by taking the gradient of the spherical harmonic expansion of the shape (1) at the location of the square. All torques are then referred back to the old coordinate system where the z-axis points along the positive rotation axis. As a check the torque from just the photons coming in from the Sun and striking the surface is computed; this torque should ideally be zero when averaged over a full rotation and asteroid year, as stated above. In practice it is usually about a factor of 10 smaller than the thermal torque, so that the accuracy of this scheme to account for shadowing is probably good only to about the 10% level.

The moment of inertia of each asteroid is also required. Here C is the moment of inertia, M is the mass, and R is the radius of each asteroid, where R is defined as the radius of a sphere which gives the volume V; i.e., $V = 4\pi R^3/3$. The angular speed is denoted by ω. The equations below use the actual moments of inertia of the asteroids, which is $C/MR^2 \cong 0.50$ for Deimos (Rubincam *et al.* 1995), 0.49 for Phobos (Chao and Rubincam 1989), 0.63 for Gaspra (Thomas *et al.* 1994), 0.89 for Eros (Yeomans *et al.* 1999; Veverka *et al.* 1999), and 0.92 for the highly elongated Ida (Thomas *et al.* 1996). The densities of Pseudo-deimos, Pseudo-phobos, Pseudo-ida, and Pseudo-eros are the same as their namesakes. The density of Gaspra is unknown, so the density of Pseudo-gaspra is conservatively assumed here to be 3 g m^{-3}, which is high compared to about 2 g m^{-3} for Phobos and Deimos (Duxbury and Callahan 1989), 1.3 g m^{-3} for 253 Mathilde (Thomas *et al.* 1997), 2.6 g m^{-3} for Ida (Belton *et al.* 1996), and 2.5 g m^{-3} for Eros (Yeomans *et al.* 1999, Veverka *et al.* 1999). The spin-up timescale is proportional to density, so that a lower density will shorten it, and a higher one will raise it. All torques have been computed using spherical harmonic expansions of shape complete to degree and order 12, except for Pseudo-deimos, which is complete to degree and order 6. It appears that Deimos' windmill shape is a large-scale property; degrees higher than 6 do not change the torques very much, so that this low value is used here.

RESULTS

The torque $\boldsymbol{\tau}_z$ along the axis of maximum moment of inertia which changes the rotation rate and the torque $\boldsymbol{\tau}_\Theta$ whichs acts to change the obliquity are shown in Fig. 3. The positive direction of the body-fixed z-axis points such that the magnitude of the torque $\boldsymbol{\tau}_z$ is positive when the z-axis is normal to the orbital plane. The angle Θ is defined such that it is the angle between the orbital plane and $\hat{\mathbf{s}}$. When the unit spin vector $\hat{\mathbf{s}}$ points in the positive z direction for small angles between the equator and the orbital plane, the asteroid speeds up, as shown in the top part of the figure. Because the torques are independent of the sense of rotation of the asteroid, the torques remain the same when $\hat{\mathbf{s}}$ is reversed, as shown in the bottom part of Fig. 3. For the prograde rotators Gaspra and Eros Θ is the same as the obliquity, while for Ida, which is a retrograde rotator speeding up from the YORP torque, Θ is 180° minus the obliquity. The torques are also independent of which way the Sun revolves around it as seen from the asteroid, as indicated by the arrows on either side of the Sun in Fig. 3.

The torques for Pseudo-gaspra and Pseudo-eros are shown as functions of Θ in Fig. 4; the same is done for Pseudo-deimos and Pseudo-ida in Fig. 5. The z-axis for Pseudo-deimos is the opposite of Deimos; for Deimos' present sense of rotation, it would spin down and not up.

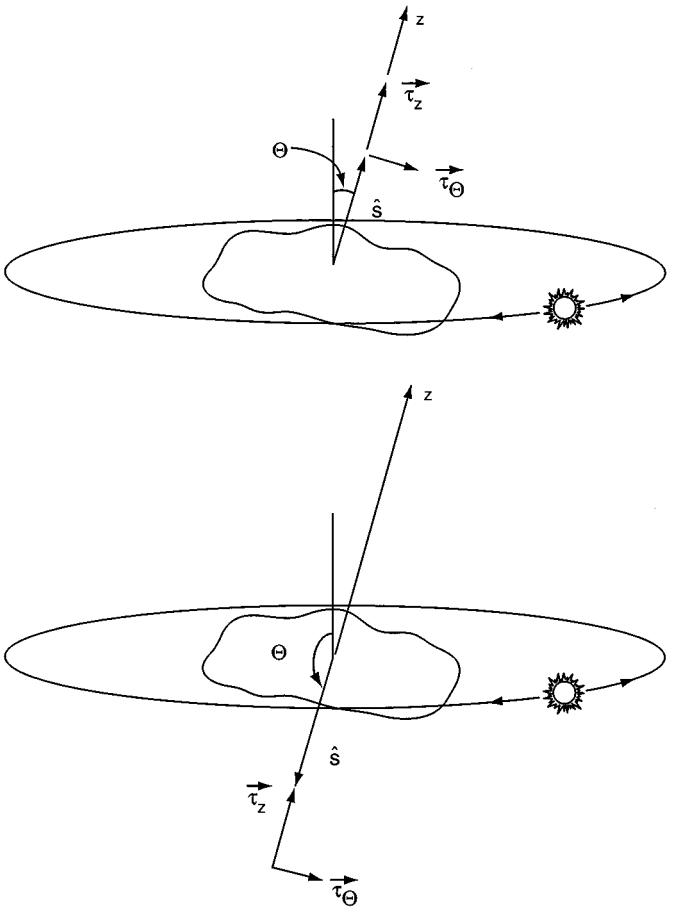

FIG. 3. Relative geometry of the asteroid and the Sun. The body-fixed z-axis of the asteroid is defined such that $\boldsymbol{\tau}_z$ points in the direction of the positive z-axis when the axis is normal to the orbital plane. The angle Θ is defined to be the angle between the unit spin vector $\hat{\mathbf{s}}$ and the the line normal to the orbital plane. For small Θ the torque $\boldsymbol{\tau}_z$ causes the asteroid to spin up, as shown in the top part of the figure. The torques are independent of the sense of the asteroid's rotation, so that when the spin is reversed the asteroid spins down, as shown in the bottom part of the figure. The torque $\boldsymbol{\tau}_\Theta$ changes the obliquity. The torques are also independent of the sense of direction of the Sun's orbit as seen from the asteroid. The magnitudes of $\boldsymbol{\tau}_z$ and $\boldsymbol{\tau}_\Theta$ are denoted by τ_z and τ_Θ, respectively.

The corresponding curves are quite similar for each object. For all the objects the rotational torque $\boldsymbol{\tau}_z$ is at its maximum when the Sun lies in the pseudo-object's equator ($\Theta = 0$). The rotational torque decreases as Θ increases but is positive for $\Theta < \sim 55^\circ$, so that the objects speed up in this regime. This torque goes to zero in the neighborhood of $\Theta \approx 55^\circ$, and for $\Theta > \sim 55^\circ$ the torque goes negative and the objects spin down. Hence these objects qualitatively behave like the simple wedges shown in Fig. 1, where it is clear that the asteroid spins up when the Sun lies in the equator, but spins down when it shines down along the rotation axis.

The torque magnitude $\boldsymbol{\tau}_\Theta$ is zero at $\Theta = 0$ and $\Theta = 90^\circ$ but is positive in between. Thus this torque acts to increase Θ, so that the objects always tend to tip over further and further. Hence an object starting out with a small value for Θ speeds up its rotation

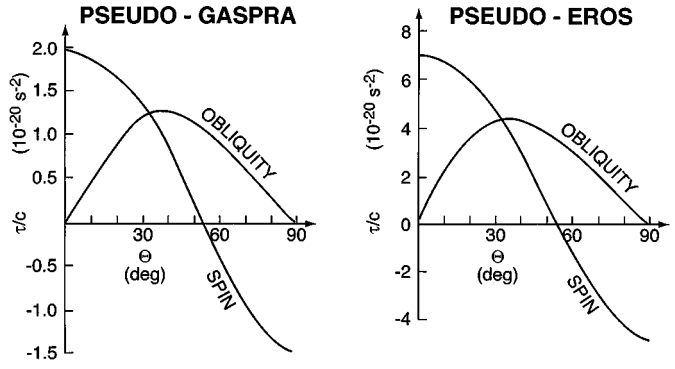

FIG. 4. The thermal torques τ divided by moment of inertia C for Pseudo-gaspra and Pseudo-eros as a function of Θ. These objects speed up for $\Theta \leq \sim 55^\circ$ and slow down for $\Theta \geq \sim 55^\circ$. The $\boldsymbol{\tau}_\Theta$ torque is always positive for $0 \leq \Theta \leq 90^\circ$, so that they always tip over further and further as time progresses.

for a while; but once it tips over far enough it slows its rotation. It turns out that $\boldsymbol{\tau}_\Theta$ for the wedges in Fig. 1 also behaves like this; hence all the objects examined here qualitatively act like the simple body shown in Fig. 1.

What about an object's behavior for $90^\circ \leq \Theta \leq 180^\circ$? For $90^\circ \leq \Theta \leq \sim 135^\circ$, an object will speed up while Θ increases. However, once Θ increases past $\sim 135^\circ$, the rotational torque points in the direction opposite to the spin as shown in the bottom part of Fig. 3, so that the object spins down. Meanwhile Θ continues to asymptotically increase toward 180°. Hence there are two states of very slow rotation: near $\Theta = 90^\circ$ and 180°, so that the spin axis is nearly perpendicular or parallel to the orbital plane.

The graph in Fig. 6 shows the time t_d it would take to double the rotation speed, so that the rotation period goes from 12 to 6 h, as a function of radius R for $\Theta = 0$, assuming the density remains the same. The doubling time is given by

$$t_\mathrm{d} = \frac{C\omega}{\tau_z}.$$

The initial angular speed ω is $2\pi/(12\ \mathrm{h}) = 1.45 \times 10^{-4}\ \mathrm{s}^{-1}$ for

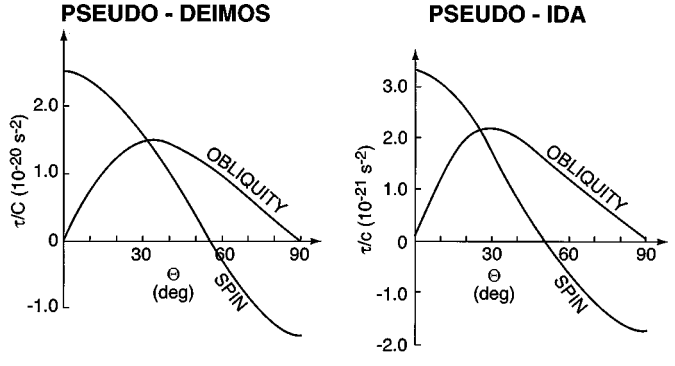

FIG. 5. The thermal torques τ divided by moment of inertia C for Pseudo-deimos and Pseudo-ida as a function of Θ. The z-axis of Pseudo-deimos is opposite that of Deimos; the real body would spin down for its present sense of rotation, rather than spin up. Pseudo-deimos is assumed to orbit the Sun at 3 AU. These two objects behave much like those in Fig. 4.

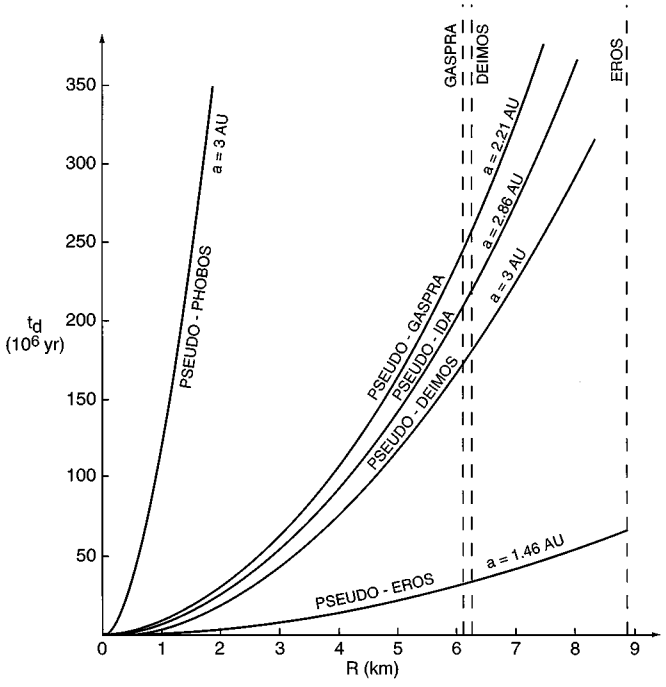

FIG. 6. Time t_d to double the rotation rate via thermal torques for five hypothetical asteroids, as a function of radius. All are assumed to be blackbodies with uniform densities in circular orbits about the Sun. Their initial rotation periods are 12 h and their obliquities are fixed at zero. Pseudo-deimos and Pseudo-phobos orbit the Sun at $a = 3$ AU, while Pseudo-gaspra is at 2.21 AU, Pseudo-eros is at 1.46 AU, and Pseudo-ida is at 2.86 AU, the respective distances of the real asteroids from the Sun. a is the semimajor axis. The dotted lines show the radii of the real Gaspra and Deimos; the radii of Phobos and Ida are off the picture. It also takes the same time t_d to slow an asteroid from 12 h to no rotation, assuming that it spins in the sense opposite to the thermal torque. This graph is meant to give an idea of the timescales; zero obliquity is actually a state of unstable equilibrium.

all objects. The curves increase with R^2 because torque behaves like area $\times$ lever arm ($R^2 \times R$), while the moment of inertia behaves like mass $\times$ radius squared ($R^3 \times R^2$). The smaller the asteroid, the more important thermal torques become. Pseudo-phobos is so symmetrical that the YORP timescale is longer than the age of the solar system and is not considered further here. The other objects, however, show a significant YORP effect on 5-km-radius objects. Ida, with its 15.7-km radius and distance of 2.86 AU from the Sun is not a good YORP candidate; but a 6-km object with Pseudo-ida's shape would spin up faster than Gaspra, even though it is further from the Sun.

Figure 6 gives the shortest possible spin-up timescale: the Sun always stands over the objects' equators in this figure, where the spin-up torque is maximal. This figure is meant merely to give an idea of the magnitude of YORP. In actuality, $\Theta = 0$ is a state of unstable equilibrium, as can be seen from the $\boldsymbol{\tau}_\Theta$ torque in Figs. 4 and 5; a small tilt will cause Θ to grow. To obtain realistic spin histories it is necessary to integrate both $\boldsymbol{\tau}_z$ and $\boldsymbol{\tau}_\Theta$.

The torques $\boldsymbol{\tau}_z$ and $\boldsymbol{\tau}_\Theta$ can be approximated by simple polynomials in Θ and the equations integrated to give spin rate ω and obliquity Θ with time:

$$\frac{d\omega}{dt} = \frac{\boldsymbol{\tau}_z}{C} \tag{6}$$

$$\frac{d\Theta}{dt} = \frac{\boldsymbol{\tau}_\Theta}{C\omega}. \tag{7}$$

The evolution of the spin states for Pseudo-gaspra is shown in Fig. 7 and for Pseudo-eros in Fig. 8. In each case the current rotation rate and obliquity were taken as initial values (marked by the dotted line in each figure) and Eqs. (6) and (7) integrated forward and backward to give ω and Θ as functions of time. The integration used a fourth-order Runge-Kutta scheme with 10^6-year step sizes. These curves show that the spin state of both

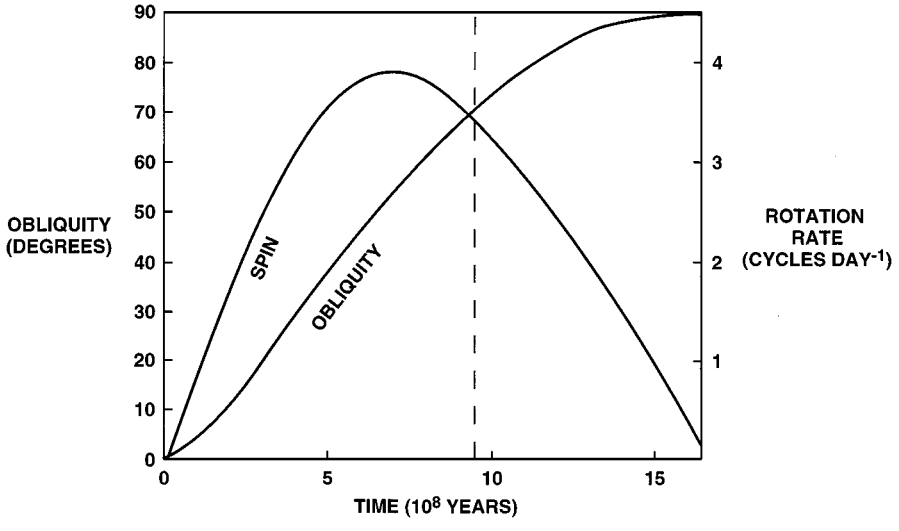

FIG. 7. The evolution of spin and obliquity for Pseudo-gaspra, assuming Gaspra's present obliquity and rotation rate. Eventually it slows down, at which point it either starts its evolution all over (the YORP cycle) or perhaps tumbles randomly.

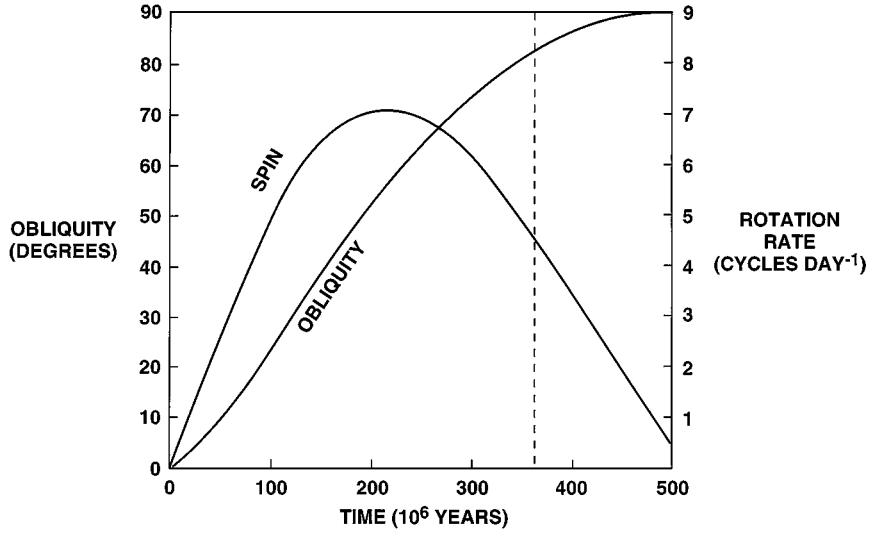

FIG. 8. The evolution of spin and obliquity for Pseudo-eros, assuming Eros' present obliquity and rotation rate.

objects can significantly evolve on a 10^8-year timescale. Pseudo-gaspra, for instance, can go from a 12-h rotation period (which is typical of many asteroids) and an obliquity of about 15°, to its peak rotation rate of nearly a 6-h period and an obliquity of 55° in 4.5×10^8 years. To go through a complete cycle of slow rotation to spin up and then back to slow rotation takes about 1.5×10^9 years. The timescale of the real asteroid may be almost twice as fast (see next section). Pseudo-eros can go from a 12-h rotation period and an obliquity of about 8° to a 6-h period and an obliquity of 40° in 40×10^6 years. To go through a complete cycle of slow rotation to spin up and then back to slow rotation takes about 5×10^8 years for Pseudo-eros.

The adequacy of the Runge-Kutta integration was checked by integrating numerically the hypothetical torques below and then comparing the output against the analytical solution. The torques are written in the form

$$\tau_z = b_0 + b_1\Theta + b_2\Theta^2 + \cdots = \sum_{i=0}^{I} b_i \Theta^i \tag{8}$$

and

$$\tau_\Theta = \frac{c\Theta}{c_0 + c_1\Theta + c_2\Theta^2 + \cdots} = \frac{c\Theta}{\sum_{j=0}^{J} c_j \Theta^j}. \tag{9}$$

Also,

$$\left(\sum_{i=0}^{I} b_i \Theta^i\right)\left(\sum_{j=0}^{J} c_j \Theta^j\right) = \sum_{k=0}^{K} d_k \Theta^k.$$

Combining (6) and (7) gives

$$\frac{\mathrm{d}\omega}{\omega} = \frac{\tau_z}{\tau_\Theta}\mathrm{d}\Theta,$$

which has the analytical solution

$$\frac{\omega}{\omega_0} = \left(\frac{\Theta}{\Theta_0}\right)^{\frac{b_0 c_0}{c}} e^{-\sum_{k=1}^{K} \frac{d_k}{kc}\Theta_0^k} e^{\sum_{k=1}^{K} \frac{d_k}{kc}\Theta^k}, \tag{10}$$

where ω_0 and Θ_0 are the initial values. The Runge-Kutta numerical solution using a 10^6-year step size for Pseudo-gaspra showed only trifling differences with the analytical solution (10), indicating a healthy integration. The coefficients b_i and c_j can be chosen to realistically represent the torques, except for τ_Θ at high obliquities; τ_Θ does not go to zero at $\Theta = 90°$ in (9). However, the analytical solution can be adapted to Θ near 90° by making a suitable change in variables from Θ to $\Theta' = 90° - \Theta$ so that τ_Θ goes to zero at 90°, and the two analytical solutions can be spliced together. The main drawback of (10) is that it does not show the YORP timescale.

COMPARISON WITH REAL ASTEROIDS

The objects investigated above are called "pseudo-asteroids" because they are idealizations of real asteroids, the intent here being only to demonstrate the probable importance of the YORP effect. It is assumed here that all the objects are blackbodies, but of course all bodies reflect some sunlight. High albedoes lessen the thermal torque: by reflecting sunlight off an asteroid, a high albedo makes less thermal energy available for reradiation. However, this loss is roughly offset by the momentum transfer from photons reflected off the surface. In specular reflection, for instance, the force is also normal to the surface, just like the thermal force. In other words, the reflective part of the YORP effect investigated by Paddack and O'Keefe works in the same direction as the thermal part of the effect presented here. The reflective torques are independent of the rotation speed, unlike the thermal torques.

The spherical harmonic shapes are smoothed representations of the real shapes. The adequacy of the smoothed shapes can be estimated by computing the rate of spin-up from the $5^\circ \times 5^\circ$ square faces on which they are based, with the Sun in the equatorial plane and only those faces that look away from the Sun assumed to be in shadow. This computation is easy to perform, but does not account for a face that points toward the Sun but is blocked from sunlight by a protrusion. In the case of Deimos a low degree and order 6 shape appears to be adequate for the YORP effect; the faces give little difference from the spherical harmonic shape. Thus it is no surprise that a more detailed degree and order 10 shape also gives trifling differences from the faces.

The agreement between the spherical harmonic and the $5^\circ \times 5^\circ$ face approach is not so good for the highly irregular Gaspra. For example, the degree and order 12 spherical harmonic shape gives a spin-up rate about 30% smaller than the faces do. Moreover, the estimated density of Pseudo-gaspra may be high (see above). Hence the YORP timescale computed here for Pseudo-gaspra may be conservatively long compared to the real Gaspra; the real asteroid may evolve at a rate perhaps twice as fast as Pseudo-gaspra. Ida gives the same result: the 12th-degree shape of Pseudo-ida is 30% slower than the faceted shape. Thus, grossly irregular shapes need either to be expanded to high degree and order, or the spherical harmonic shapes should be abandoned for the face approach. The latter will require a proper accounting of shadows such as performed by Sazanov (1994) and Komarov and Sazanov (1994).

It should also be noted that the shape of a real asteroid would not be expected to remain constant over time as it is sculpted by impacts. Thus the magnitude and even sign of the YORP effect may not be constant over time.

The pseudo-asteroids are all assumed to be homogeneous in density. This assumption is consistent with the small bodies whose shapes and rotation axes are well determined (Chao and Rubincam 1989, Thomas *et al.* 1994, 1996, Rubincam *et al.* 1995, Veverka *et al.* 1999). Presumably asteroids with significant density inhomogeneities do exist, but what fraction of the general population of small asteroids they constitute is unknown. The inhomogeneity affects the center of mass position, which in turn affects the thermal torque calculation.

Regoliths are assumed in the calculations here, coming in through the thermal fudge factor $f_{\rm th}$. Regoliths help the YORP effect because of their poor thermal conductivity compared to bare rock or iron. Regoliths enhance the day–night temperature difference needed for this effect; a lunar-like regolith has a thermal skin depth only $\sim$0.5 cm deep at typical rotation frequencies of a few hours (e.g., Rubincam 1995, p. 1587), so that a regolith depth of $\sim$1 cm or so is all that is required to produce a large effect. Bare rock or iron can reduce the YORP effect by an order-of-magnitude or more. Further, a high rotation speed lessens the thermal torque by smoothing out the day–night differences, while a low rotation speed enhances YORP.

DISCUSSION

Four out of the five objects investigated here show significant windmill factors, with only Phobos being too symmetrical for much of a YORP effect. While the statistics are small, they indicate that YORP may be active on a large fraction of the smaller asteroids. Of particular interest is the YORP cycle. For the objects investigated here, though they may speed up for a while, they ultimately slow down as their obliquities asymtoptically approach 90°. The results here suggest that while Gaspra and Eros are fast rotators, both have passed their peak rotation speeds and are currently slowing down. It is interesting to note that Figs. 6 and 7 indicate that both objects stay below the rubble-pile fission limit of about 10 cycles day^{-1} (Harris 1996) in their YORP evolution. 1566 Icarus is also a fast rotator (e.g., McFadden *et al.* 1989), and YORP may have something to do with its very speedy 2.3-h spin period.

On the other hand, 253 Mathilde is a slow rotator. While Mathilde may be a YORP candidate, with its relatively large size and probable frequent impacts in the asteroid belt, its slow rotation might be difficult to explain solely with YORP (Veverka *et al.* 1997). However, it may have despun by impacts or losing a satellite and then slowed further to its present 17-day period by thermal torques. Unfortunately, the shape of Mathilde is unknown; only one side of it has been seen (Thomas *et al.* 1997).

One can speculate that once an object spins slowly enough it starts to tumble due to YORP and gravitational torques from the Sun; 4179 Toutatis, an asteroid 2 km in radius with a several-day tumbling period, may be an example (Ostro *et al.* 1995, Hudson and Ostro 1995, Harris 1994). Random tumbling will shut off the YORP effect. In some cases of tumbling principal axis rotation may then eventually reestablish itself through internal dissipation with the spin axis canted at some arbitrary obliquity, at which time YORP again operates, starting the cycle all over.

How does the YORP effect compare with impacts in changing the spin states of small asteroids? Farinella *et al.* (1998) find that the characteristic time $t_{\rm rot}$ to substantially change the rotation period of an asteroid in the main belt is approximately

$$t_{\rm rot} \cong 3.34 \times 10^6 \text{ years} \left(\frac{R}{1m} \right)^{\frac{1}{2}}.$$

For a Gaspra-sized object this is about 250×10^6 years, so that the YORP timescale is comparable to collisions for this size range. For smaller objects it becomes more favorable for YORP due to the R^2 dependence of the YORP timescale compared to the $R^{\frac{1}{2}}$ dependence assumed for collisions. At $R = 1$ km, the YORP cycle for Pseudo-gaspra would take 40×10^6 years, while Pseudo-eros would take only 6.5×10^6 years.

YORP can be expected to completely dominate collisions in the inner Solar System for $R <$ 5-km asteroids, due to their small size, increased insolation, and smaller population of impactors compared to the main belt. YORP should also dominate spin

changes from tidal encounters (Bottke *et al.* 1997, Richardson *et al.* 1998) in the inner Solar System for $R < 1$ km. W. F. Bottke (pers. commun. 1999) finds that the average time between spin-changing tidal encounters with Earth and Venus is about 13 million years, longer than the ∼few million years for YORP for these objects.

The limiting factor on YORP in the inner Solar System may be the lifetime of the NEAs (near-Earth asteroids). Recent results by Gladman *et al.* (1997, Fig. 2) indicate that NEAs have a half-life of about 10 million years before they impact a planet or the Sun, or are ejected from the Solar System by Jupiter.

Eros, however, may be a collision fragment tens of millions of years old (Michel *et al.* 1996, W. Bottke pers. commun. 1998), long enough to be significantly affected by YORP. In fact, with its high obliquity, Eros could be a highly evolved YORP object. The laser altimeter on board the NEAR (Near Earth Asteroid Rendezvous) mission will determine its shape more accurately than the currently available model, and the orbit of the spacecraft will fix its center of mass by recovering its gravitational field, so that a much better YORP calculation will be possible; but the YORP deceleration is probably too small to be detected over NEAR's lifetime (David E. Smith, pers. commun. 1999).

All the calculations assume principal axis rotation, so that dissipation inside the pseudo-asteroids is assumed to be high enough to keep them in that state. Harris (1994), following McAdoo and Burns (1974) and Burns and Safronov (1973), finds that the characteristic time $t_{\rm PA}$ for returning a tumbling asteroid to principal axis rotation is $t_{\rm PA} \approx P^3/(20R^2)$, where P is the period of rotation in hours, R is the radius in kilometers, and $t_{\rm PA}$ is in millions of years. For 5-km-radius asteroids rotating with 12 h periods $t_{\rm PA}$ is about 3 million years, shorter than the YORP timescale of ∼100 million years for the objects considered here, so that they should remain close to principal axis rotation.

The YORP torques may inspire nonprincipal axis rotation if the dissipation timescale is longer than the YORP timescale, as expected for the smaller objects. For example, for a 1-km asteroid $t_{\rm PA}$ is about 86 million years, which is longer than the YORP timescales of 40 million years for a 1-km Pseudo-gaspra and 6.5 million years for a 1-km Pseudo-eros. This aspect of YORP, which would involve integrating the Euler angles (Sazanov 1994, Komarov and Sazanov 1994) remains to be investigated. Because YORP is straightforward physics applied to irregular shapes, it is likely that YORP is operative on these smaller objects; since they are generally found to be in principal axis rotation, then YORP may not inspire much tumbling, or internal dissipation in them may be higher than expected.

Small asteroids ($R < 5$ km) exhibit an excess of fast and slow rotators compared to a Maxwellian distribution (Pravec *et al.* 1997, Harris 1996). Given the expected YORP dominance at these sizes in the main belt and at smaller sizes in the near-Earth region, it may be that YORP is responsible for this bimodal distribution of fast and slow spin rates by depopulating the center and populating the extremes (W. F. Bottke, pers. commun. 1998).

YORP may also profoundly affect the rotation of meteoroids. A basaltic meteoroid 1 m in radius with Gaspra's shape and no regolith would shorten a 12-h spin period to 6 h on the 10^3- to 10^4-year timescale. With cosmic ray exposure ages typically of 20 million years, substantial changes in spin rate might be expected for slow rotators. Fast rotators would be less affected by thermal torques but would still experience the reflective torque. In an approximate calculation of the reflective torque, a dark meteoroid with the shape of Pseudo-gaspra, Gaspra's obliquity and distance from the Sun, an albedo of 0.05, and a spin period of 20 s, for instance, has a YORP cycle of about 10^6 years (see Fig. 9), which is still a factor of ∼20 faster than the cosmic ray exposure ages. So regardless of rotation speed, YORP might

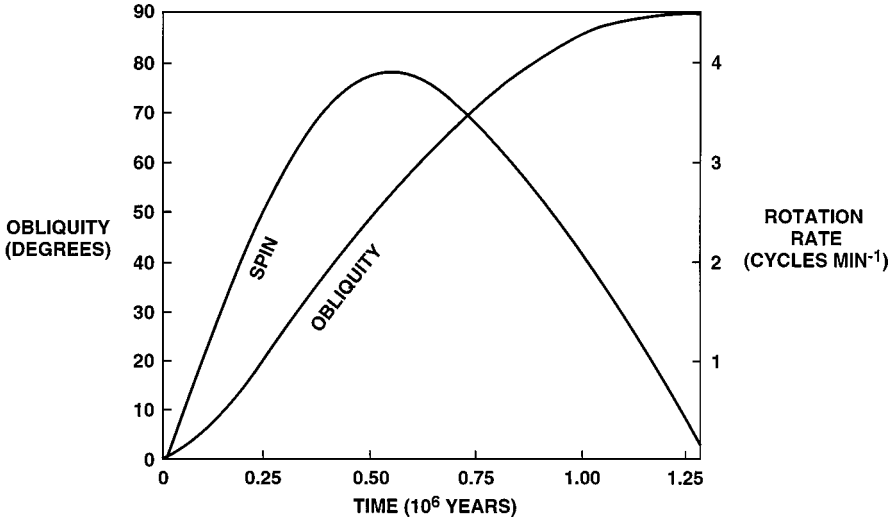

FIG. 9. The approximate evolution of spin and obliquity of a 1-m-radius meteoroid for the reflective YORP torque, assuming Pseudo-gaspra's shape, density, obliquity, and distance from the Sun, an albedo of 0.05, and a rotation period of 20 s. The shape of the curves is the same as in Fig. 6; only the timescale has changed.

greatly affect the presumed Yarkovsky orbit evolution of meteoroids (e.g., Peterson 1976, Rubincam 1995, Farinella *et al.* 1998, and Bottke *et al.* 2000). A meteoroid might go through many YORP cycles; or it might tumble randomly, shutting off the YORP effect until principal axis rotation is reestablished.

The reflective part of YORP was invoked by Paddack (1969, 1973), Paddack and Rhee (1975), and O'Keefe (1976) to spin up centimeter-sized meteoroids to rotational bursting. The idea was that secular spin up would continue until the centrifugal force overcame the strength of the meteoroid, at which point it would fracture and fly apart. Their intent was to show that tektites had to originate within the Earth–Moon system; further away (Mars, for example) would mean a transit time long compared to the spin-up timescale, so that most of the tektities would fragment before they reached Earth. The fact that most appeared intact argued for a nearby source.

The results obtained here indicate that rotational bursting may not happen very often. The reason is that the obliquity torque is an inevitable accompaniment of the rotational torque. Even if the spin vector is normal to or lies in the orbital plane, the state is unstable and a small perturbation will start the tilt increasing; when the meteoroid tips over far enough the rotational torque will go negative and the spin will slow. Hence, meteoroids may be constantly speeding up and slowing down with the YORP cycle (assuming principal axis rotation), or tumbling, instead of speeding up to bursting.

It may also be that the evolution through the YORP cycle might be interrupted by objects entering special YORP spin states. For instance, an asteroid with a thermal inertia which varies across the surface might cause the rotational torque to go to zero at a particular rotation rate, so that the rotational speed remains constant thereafter. Special spin states and other aspects of YORP are currently under investigation.

ACKNOWLEDGMENTS

I thank William Bottke for numerious criticisms, comments, and calculations which greatly improved the paper. I thank John A. O'Keefe, David E. Smith, and Clark Chapman for enlightening discussions and Peter C. Thomas for the numerical shapes of Gaspra, Deimos, Phobos, and Ida. Yanping Guo supplied the shape of Eros to Mark Torrence, who gave it to me. I thank Susan Poulose for expert programming and Bruce G. Bills for spherical harmonic rotation subroutines. Stuart Weidenschilling, Alan Harris, Joseph A. Burns, Stan Love, Paolo Paolicchi, and an anonymous referee made well-directed criticisms. Vladislav Sidorenko brought the papers of V. V. Sazanov and coauthors to my attention. I have added the names of John A. O'Keefe and Stephen J. Paddack to what they call the Yarkovsky-Radzievskii effect; O'Keefe and Paddack were instrumental in realizing that shape and thermal radiation play important roles in radiative torques. Radzievskii concentrated on albedo differences. This paper is dedicated to the late John A. O'Keefe.

REFERENCES

Belton, M. J. S., C. R. Chapman, K. P. Klaasen, A. P. Harch, P. C. Thomas, J. Veverka, A. S. McEwen, and R. T. Pappalardo 1996. Galileo's encounter with 243 Ida: An overview of the imaging experiment. *Icarus* **120**, 1–19.

Binzel, R. P., P. Farinella, V. Zappala, and A. Cellino 1989. Asteroid rotation rates: Distributions and statistics. In *Asteroids II* (R. P. Binzel, T. Gehrels, and M. S. Matthews, Eds.), pp. 416–441. Univ. of Arizona Press, Tucson.

Bottke, W. F., D. C. Richardson, and S. Love 1997. Can tidal disuption of asteroids make crater chains on the Earth and Moon? *Icarus* **126**, 470–474.

Bottke, W. F., D. P. Rubincam, and J. A. Burns 2000. Dynamical evolution of main belt meteoroids: Numerical simulations incorporating planetary perturbations and Yarkovsky thermal forces. *Icarus* **145**, 301–331.

Burns, J. A., and V. S. Safronov 1973. Asteroid nutation angles. *Mon. Not. R. Astron. Soc.* **165**, 403–411.

Chao, B. F., and D. P. Rubincam 1989. The gravitational field of Phobos. *Geophys. Res. Lett.* **16**, 859–862.

Davis, D. R., S. J. Weidenschilling, P. Farinella, P. Paolicchi, and R. P. Binzel 1989. Asteroidal collisional history: Effect on sizes and spins. In *Asteroids II* (R. P. Binzel, T. Gehrels, and M. S. Matthews, Eds.), pp. 805–826. Univ. of Arizona Press, Tucson.

Duxbury, T. C., and J. D. Callahan 1989. Phobos and Deimos control networks. *Icarus* **77**, 275–286.

Farinella, P., D. Vokrouhlicky, and W. K. Hartmann 1998. Meteorite delivery via Yarkovsky orbital drift. *Icarus* **132**, 378–387.

Gladman, B. J., F. Migliorini, A. Morbidelli, V. Zappala, P. Michel, A. Cellino, C. Froeschle, H. F. Levison, M. Bailey, and M. Duncan 1997. Dynamical lifetimes of objects injected into asteroid belt resonances. *Science* **277**, 197–201.

Harris, A. J. 1994. Tumbling asteroids. *Icarus* **107**, 209–211.

Harris, A. J. 1996. The rotation rates of very small asteroids: Evidence for "rubble-pile" structure. *Lun. Planet. Sci. Conf. 27th*, 493–494.

Hudson, R. S., and S. J. Ostro 1995. Shape and non-principal axis spin state of asteroid 4179 Toutatis. *Science* **270**, 84–86.

Komarov, M. M., and V. V. Sazanov 1994. Light pressure forces and torques exerted on an asteroid of arbitrary shape. *Sol. Syst. Res.* **28**, 16–23.

Lebofsky, L. A., and J. R. Spencer 1989. Radiometry and thermal modeling of asteroids. In *Asteroids II* (R. P. Binzel, T. Gehrels, and M. S. Matthews, Eds.), pp. 128–147. Univ. of Arizona Press, Tucson.

McAdoo, D. C., and J. A. Burns 1974. Approximate axial alignment times for spinning bodies. *Icarus* **21**, 86–93.

McFadden, L., D. J. Tholen, and G. J. Veeder 1989. Physical properties of Aten, Apollo and Amor asteroids. In *Asteroids II* (R. P. Binzel, T. Gehrels, and M. S. Matthews, Eds.), pp. 442–467. Univ. of Arizona Press, Tucson.

Michel, P., C. Froeschle, and P. Farinella 1996. Dynamical evolution of two near-Earth asteroids to be explored by spacecraft: (433) Eros and (4660) Nereus. *Astron. Astrophys.* **313**, 993–1007.

O'Keefe, J. A. 1976. *Tektites and Their Origin*. Elsevier, New York.

Ostro, S. J., and R. S. Hudson, R. F. Jurgens, K. D. Rosema, D. B. Campbell, D. K. Yeomans, J. F. Chandler, J. D. Giorgini, R. Winkler, R. Rose, S. D. Howard, M. A. Slade, P. Perillat, and I. I. Shapiro 1995. Radar images of asteroid 4179 Toutatis. *Science* **270**, 80–83.

Paddack, S. J. 1969. Rotational bursting of small celestial bodies: Effects of radiation pressure. *J. Geophys. Res.* **74**, 4379–4381.

Paddack, S. J. 1973. *Rotational Bursting of Small Celestial Bodies.* Ph.D. thesis, Catholic University, Washington, D.C.

Paddack, S. J., and J. W. Rhee 1975. Rotational bursting of interplanetary dust particles. *Geophys. Res. Lett.* **2**, 365–367.

Peterson, C. 1976. A source mechanism for meteorites controlled by the Yarkovsky effect. *Icarus* **29**, 91–111.

Pravec, P., M. Wolf, L. Sarounova, S. Mottola, A. Erikson, G. Hahn, A. W. Harris, A. W. Harris, and J. W. Young 1997. The near-Earth objects follow-up program. II. Results for 8 asteroids from 1982 to 1995. *Icarus* **130**, 275–286.

Radzievskii, V. V. 1954. A mechanism for the disintegration of asteroids and meteorites. *Dokl. Akad. Nauk SSSR* **97**, 49–52.

Richardson, D. C., W. F. Bottke, and S. G. Love 1998. Tidal distortion and disruption of Earth-crossing asteroids. *Icarus* **134**, 47–76.

Rubincam, D. P. 1987. LAGEOS orbit decay due to infrared radiation from Earth. *J. Geophys. Res.* **92**, 1287–1294.

Rubincam, D. P. 1995. Asteroid orbit evolution due to thermal drag. *J. Geophys. Res.* **100**, 1585–1594.

Rubincam, D. P., B. F. Chao, and P. C. Thomas 1995. The gravitational field of Deimos. *Icarus* **116**, 63–67.

Sazanov, V. V. 1994. Motion of an asteroid about its center of mass due to torque from light pressure. *Sol. Syst. Res.* **28**, 152–162.

Tedesco, E. F. 1989. Asteroid magnitudes, UBV colors, and IRAS albedos and diameters. In *Asteroids II* (R. P. Binzel, T. Gehrels, and M. S. Matthews, Eds.), pp. 1090–1138. Univ. of Arizona Press, Tucson.

Thomas, P. C., M. J. S. Belton, B. Carcich, C. R. Chapman, M. E. Davis, R. Sullivan, and J. Veverka 1996. The shape of Ida. *Icarus* **120**, 20–32.

Thomas, P. C., J. Veverka, J. Bell, C. Chapman, M. Malin, L. McFadden, S. Murchie, and M. Robinson 1997. Asteroid Mathilde: Geodesy and geology from NEAR multispectral imagaing data (abstract). *Eos Trans. AGU* **78** (46, Fall Meeting suppl.), F400.

Thomas, P. C., J. Veverka, D. Simonelli, P. Helfenstein, B. Carcich, M. J. S. Belton, M. E. Davies, and C. Chapman 1994. The shape of Gaspra. *Icarus* **107**, 23–36.

Veverka, J., and 28 colleagues 1997. NEAR's encounter with 253 Mathilde: The first look at a C-type asteroid, *Eos Trans. AGU* **78** (46, Fall Meeting suppl.), F400.

Veverka, J., P. C. Thomas, J. F. Bell, M. Bell, B. Carcich, B. Clark, A. Harch, J. Joseph, P. Martin, M. Robinson, S. Murchie, N. Izenberg, E. Hawkins, J. Warren, R. Farquhar, A. Cheng, D. Dunham, C. Chapman, W. J. Merline, L. McFadden, D. Wellnitz, M. Malin, W. M. Owen, J. K. Miller, B. G. Williams, and D. K. Yeomans 1999. Imaging of asteroid 433 Eros during NEAR's flyby reconnaissance. *Science* **285**, 562–564.

Yeomans, D. K., P. G. Antreasian, A. Cheng, D. W. Dunham, R. W. Farquhar, R. W. Gaskell, J. D. Giorgini, C. E. Helfrich, A. S. Konopliv, J. V. McAdams, J. K. Miller, W. M. Owen, P. C. Thomas, J. Veverka, and B. G. Williams 1999. Estimating the mass of asteroid 433 Eros during the NEAR spacecraft flyby. *Science* **285**, 560–561.